

## Effect of aluminum content on the properties of lanthana-supported nickel catalysts to WGSR

Manuela de S. Santos<sup>a</sup>, Guillermo Paternina Berrocal<sup>a</sup>, José Luís Garcia Fierro<sup>b</sup>,  
Maria do Carmo Rangel<sup>a\*</sup>

<sup>a</sup>*Instituto de Química, Universidade Federal da Bahia. Campus Universitário de Ondina, Federação. 40 170-280, Salvador, Bahia, Brazil. \*E-mail: mcarmov@ufba.br*

<sup>b</sup>*Instituto de Catálisis y Petroquímica, CSIC, Cantoblanco, 28049, Madrid, Spain*

The effect of aluminum content on the properties of lanthana-supported nickel catalysts was evaluated in this work, in order to find new catalysts for water gas shift reaction (WGSR). It was noted that small amounts of aluminum increased the specific surface and the activity and thus is benefic to the catalyst. However, high amounts of aluminum causes a decrease on both properties and this was assigned to a strong interaction between nickel and aluminum, which stabilizes the Ni<sup>2+</sup> species on the surface and makes the production of the active phase (metallic nickel) more difficult.

### 1. Introduction

The search for processes to obtain high pure hydrogen has increased in recent years, due to its large importance as fuel and for the production of other high value products. From the commercial point of view, the most important route to produce hydrogen is the steam reforming of natural gas. However, this reaction also produces carbon monoxide that can poison most of metallic catalysts. In order to remove these products from the gaseous stream, and also to increase the hydrogen production, most of industrial plants have another unit in which carbon monoxide is converted to carbon dioxide, which is removed from the stream in a further step [1]. The oxidation of carbon monoxide to carbon dioxide is carried out in the presence of steam and is known as water gas shift reaction (WGSR). In order to achieve rates for commercial purposes, this

reaction is often performed in two steps in industrial processes. The first one, called high temperature shift (HTS), occurs in the range of 320 at 450°C in favorable kinetic conditions, while the second step (low temperature shift, LTS) at 200 to 250°C is favored by thermodynamics [1-3].

The commercial catalysts used in the HTS reaction comprise hematite ( $\alpha$ - $\text{Fe}_2\text{O}_3$ ), containing chromium oxide among other dopants. In commercial processes, this solid is reduced in situ, producing magnetite ( $\text{Fe}_3\text{O}_4$ ), which is believed to be the active phase. This catalyst is very active and selective and is resistant against several poisoning; besides, it has a low cost. However, they have the inconvenience of being toxic, due to the chromium compounds and also of deactivating with time, due to the decrease of the specific surface area [2-5]. These features have motivated several studies addressed to new catalysts. In this work, lanthana-supported nickel catalysts (with aluminum or not) were studied with the aim of developing new catalysts to HTS reaction. These solids have the advantage of being chromium-free and the support can also prevent the deactivation of the active phase.

## 2. Experimental

The support (lanthana) was prepared by adding a lanthanum nitrate solution (250 mL, 1 M) and 250 mL of 8.5% (v/v) of an ammonium hydroxide solution to a beaker with water, at room temperature. After the addition of the reactants, the system was kept under stirring for 24 h and then centrifuged (2500 rpm, 4 min). The gel was dried in oven at 120 °C, for 24 h, ground and sieved in 80 mesh and heated under air flow at 550 °C, for 4 h. This solid was named L sample. In the preparation of the LA10 sample ( $\text{La}/\text{Al}$  (molar)= 10), 250 mL of aluminum nitrate solution (0.1 M) and lanthanum nitrate (1 M) were used while to get the sample with  $\text{La}/\text{Al} = 1$ , an aluminum nitrate solution 1 M was used. The catalysts with 10% of nickel were prepared by wet impregnation of a nickel nitrate solution on pure lanthanum oxide or aluminum-doped ones, using 1.4 mL of the nickel nitrate solution ( $3.4 \text{ mol.L}^{-1}$ ) per gram of the support. The solution was kept in contact with the support for 24 h, at room temperature and then filtered and dried in oven at 120 °C, for 24 h. The samples were heated under air flow, for 3 h at 600 °C, producing NL, NLA10 and NLA1 samples. The support precursors were characterized by thermogravimetry (TG) and the supports and the catalysts was analyzed by specific surface area measurements, X-ray diffraction (XRD), temperature programmed reduction (TPR), chemical analysis and X-ray photoelectron spectroscopy (XPS). After the reaction, the catalysts were analyzed by XRD, specific surface area measurements and XPS. The elemental analysis of the solids was determined by flame atomic absorption spectrometry using a SpectrAA 220 Varian equipment. The sample (0.005 g)

was previously dissolved in a mixture of hydrochloric acid and nitric acid (3:1). The XRD was performed at room temperature with a Shimadzu model XRD 6000 instrument, using  $\text{CuK}\alpha$  radiation generated at 40 kV and a nickel filter. The specific surface areas were measured in a Micromeritics model TPR/TPO 2900 equipment on samples previously heated under nitrogen (160 °C, 1 h). The samples were analyzed with a 30%  $\text{N}_2/\text{He}$  mixture. The temperature programmed reduction was performed in the same equipment, using a 5%  $\text{H}_2/\text{N}_2$  mixture (60  $\text{mL}\cdot\text{min}^{-1}$ ) at a heating rate of 10 ° $\cdot\text{min}^{-1}$ . The solid was heated up to 1000 °C and the consumption of hydrogen was measured by a thermal conductivity detector. X-ray photoelectron spectra were obtained with a VG Escalab 220R spectrometer equipped with a  $\text{MgK}\alpha$  X-ray radiation source ( $h\nu=1253.6$  eV) and a hemispherical electron analyzer.

The catalyst performance was evaluated using 0.15 g of catalyst powder (100 mesh) and a fixed-bed microreactor. The experiments were carried out under isothermal condition (370 °C) and at atmospheric pressure, employing a steam to process gas molar ratio of 0.6. These conditions were chosen to get 10% of conversion, using a commercial catalyst. A standard mixture containing 9.82% CO, 9.70%  $\text{CO}_2$ , 19.67%  $\text{N}_2$  and  $\text{H}_2$  (balance) was used as process gas. The reaction products were analyzed by gas chromatography, using a CG-35 instrument with Porapak Q and molecular sieve columns.

### 3. Results and Discussion

The X-ray diffractograms of the supports (not shown) displayed peaks of the lanthanum oxide,  $\text{La}_2\text{O}_3$  ( JCPDS 05-0602) and of the orthorhombic lanthanum nitrate hydroxide,  $\text{La}(\text{OH})_2\text{NO}_3$  (JCPDS 26-1144), except for the solid with  $\text{La}/\text{Al}=1$  that showed an amorphous halo. The production of lanthana was confirmed by DTA and TG curves, which showed a peak at about 500 °C, followed by a weight loss. No aluminum-containing phase was detected for the LA1 sample, a fact which can be assigned to its poor crystallinity [6]. Figure 1 shows the X-ray diffractograms of the catalysts before and after the WGSR. In fresh catalysts, a mixed phase of lanthanum and nickel oxide,  $\text{La}_2\text{NiO}_4$  (JCPDS 80-1346) and lanthanum oxide,  $\text{La}_2\text{O}_3$  ( JCPDS 05-0602), besides nickel oxide, NiO (JCPDS 44-1159) and lanthanum nitrate hydroxide,  $\text{La}(\text{OH})_2\text{NO}_3$  (JCPDS 26-1146), were detected. During the WGSR, nickel oxide changed to metallic nickel (JCPDS 87-0712), while the other phases remained in the solids. The sample with the highest amount of aluminum (NLA1) remained amorphous to X-ray even after the reaction.

The specific surface areas are shown in Table 1. The addition of small amounts of aluminum to lanthana caused an increase of specific surface area from 12 (L) to 28  $\text{m}^2\cdot\text{g}^{-1}$  (LA10), indicating that it acts as a textural promoter. However, the

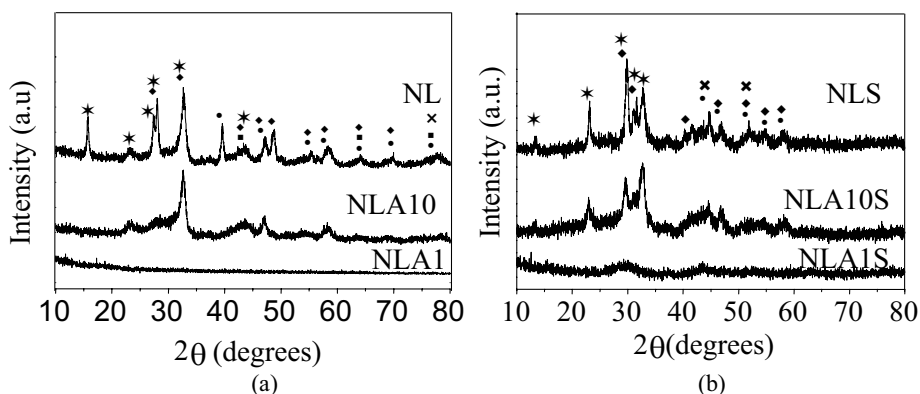


Figure 1. X-ray diffractograms of (a) fresh and (b) spent catalysts. NL sample: lanthana-supported nickel. LA10 and LA1 samples: nickel on aluminum-doped lanthana with La/Al (molar)=10 and 1, respectively. S= spent catalysts. •  $\text{La}_2\text{O}_3$ ; ▪  $\text{NiO}$ ; •  $\text{La}_2\text{NiO}_4$ ; \*  $\text{La}(\text{OH})_2\text{NO}_3$ ; ✕  $\text{Ni}^0$ .

Table1.

Specific surface areas of the catalysts (Sg), binding energies of characteristic core levels of lanthanum, aluminum and nickel and surface composition of fresh catalysts. NL sample: lanthana-supported nickel; NLA10 and NLA1: nickel supported on aluminum-doped lanthana with La/Al (molar)= 10 and 1.

Samples	Sg ( $\text{m}^2\cdot\text{g}^{-1}$ )	La3d <sub>5/2</sub>	Al2p	Ni2p 1/2	Ni / (Al+La) (surface)	Ni / (Al+La) (bulk)
NL	11	834.8	--	871.5	1.69	0.28
NLA10	15	834.8	73.7	871.8	1.15	0.28
NLA1	6.0	834.9	73.7	871.9	2.92	0.28

addition of higher amounts of aluminum (LA1) caused a decrease ( $9.0 \text{ m}^2\cdot\text{g}^{-1}$ ). The addition of nickel did not change the specific surface area for the sample without aluminum but decreased for the other samples; this can be related to the production of amorphous aluminum compounds, not detectable by XRD, but related to a large peak in DTA curves in the range of 600-950 °C.

The binding energies (BE) of some characteristic core levels of lanthanum, nickel, aluminum and nickel are displayed in Table 1. The BE for lanthanum (834.8 eV) is characteristic of  $\text{La}^{3+}$  species [7] and was the same in all species, indicating they are in the same chemical environment. The same behaviour was noted regarding the BE values for aluminium and nickel, which are typical of  $\text{Al}^{3+}$  and  $\text{Ni}^{2+}$  species, respectively [7]. The solid surface composition, expressed

as atomic ratio, is also shown in Table 1. It can be noted that the amount of nickel was higher on the surface than in the bulk for all samples. The NLA1 sample is the richest in nickel, among the samples.

The TPR profiles of the supports (not shown) displayed two peaks, which were shifted to higher temperatures, due to the addition of small amounts of aluminum (LA10). By adding higher amounts of this metal (LA1), they overlapped at an intermediate temperature, suggesting a strong interaction between aluminum and the support. These peaks are also assigned to nitrate species and lanthana reduction [8,9]. The presence of nitrate species in the solids was confirmed by XPS. As expected, the reduction profiles of the catalysts are quite different as compared to the support ones (Figure 2a). A low temperature peak (around 230 °C) appeared, which was assigned to the reduction of nickel oxide particles in weak interaction with the support [10]; this peak is absent in the sample with the highest amount of aluminum (NLA1), indicating that all nickel are in medium or strong interaction with the support. The NL and NLA1 curves also showed three other peaks above 400 °C, the first related to reduction of nickel in strong interaction with the support and the others associated with the reduction of  $\text{La}_2\text{NiO}_4$  compound. These peaks are also related to the reduction of nitrate species and of lanthanum oxide [8,9]. The addition of more aluminum (NLA1 sample) caused the overlapping of these peaks and shifted them to higher temperature, indicating that this dopant made all these reduction processes more difficult, probably due to the reduction of aluminum-based compounds (not detectable by XRD). It means that there is a strong interaction among the metals for the NLA1 sample.

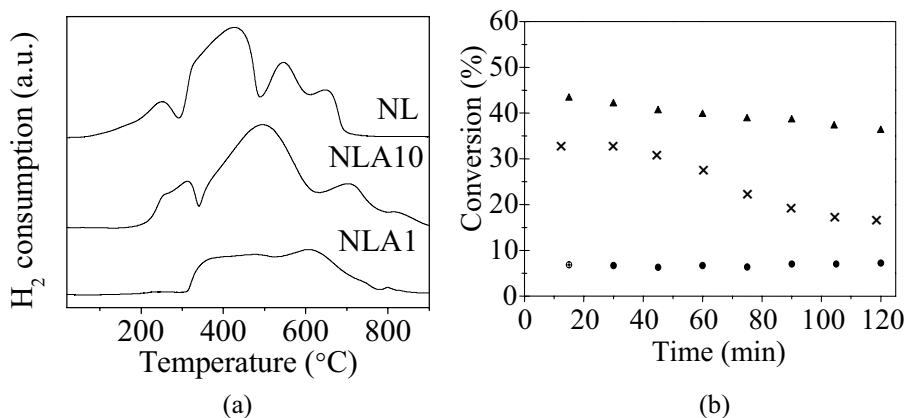


Figure 2. (a) TPR curves of the catalysts. (b) Carbon monoxide conversion as a function of time. × NL sample (lanthana-supported nickel); ▲ NLA10 and • NLA1: with La/Al (molar)= 10 and 1, respectively.

All catalysts were active in HTS reaction, as shown in Figure 2b. The pure and doped-lanthana did not show any activity, indicating that nickel is the active phase. When small amounts of aluminum were added to the catalysts, the activity strongly increased reaching a value close to the equilibrium value (46%). However, it decreased sharply when larger amounts of aluminum were added. This can be assigned to the strong interaction between nickel and the support [11-13], since the surface is rich in aluminum for this sample. Therefore, although this sample contains the largest amount of nickel on the surface most of the species are stabilized as  $\text{Ni}^{2+}$  and can not go into reduction to produce the active phase (metallic nickel). The presence of aluminum also made the catalysts more stable under the reaction condition, as shown in Figure 2b.

#### 4. Conclusions

Lanthana-supported nickel is an efficient catalyst for WGS. When small amounts of aluminum are added to this solid, no other phase is noted, besides those detected in undoped solid, but the specific surface area and the activity in WGS increase. However, the further addition of aluminum causes a sharp decrease of specific surface area and in activity, a fact which can be assigned to strong interaction among nickel, lanthana and aluminum, as detected by TPR. This stabilizes the  $\text{Ni}^{2+}$  species and makes the production of active phase (metallic nickel) more difficult, causing a decrease in catalytic activity.

#### References

1. C. Fukuhara, H. Ohkura, K. Gonohe, A. Igarashi, *Appl. Catal A: Gen.* 279 (2005) 195.
2. V. Twigg, M. V. Loyd, D. E. Ridler, *Catalyst Handbook*, Wolfe Publishing, 1989.
3. D. S. Newsome, *Catal Rev-Sci Eng.* 21(1980) 275.
4. M. I. Temkim, *Adv. Catal.*, 28 (1979) 263.
5. I. J. Lima, J. Millet, M. Aouine, M. C. Rangel, *Appl. Catal A: Gen.* 283 (2005) 91.
6. H.P. Klug, L.E. Alexander, *X-Ray Diffraction Procedures*, A Wiley-Interscience Publication.
7. C. D. Wagner, W. M. Riggs, L. E. Davis, J. F. Moulder, G. E. Muilenberg, *Handbook of X-Ray Photoelectron Spectroscopy*, Perkin-Elmer Cooperation Eden Prairie, 1978.
8. S. Ho, T. Chou, *Ind. Eng. Chem. Res.* 34 (1995) 2279.
9. A. Jones, B. McNicol, *Temperature-Programmed Reduction for Solid Materials Characterization*, Marcel Dekker, Inc. New York, 1986.
10. E. Ruckenstein, Y. H. Hu, *J. Catal.*, 161 (1996) 55.
11. M. Parvary, S. H. Jazayeri, A. Taeb, C. Petit, A. Kiennemann, *Catalysis Communications*, 2 (2001) 357.
12. Z. Xu, Y. Li, J. Zhang, L. Chang, R. Zhou, Z. Duan, *Appl. Catal A: Gen.* 210 (2001) 45.
13. S. Wang, G. Q. Lu, *Appl. Catal A: Gen.* 169 (1998) 271.